Title
COLLECTIVE MODEL DESCRIPTION OF TRANSITIONAL ODD-A NUCLEI II. COMPARISON WITH UNIQUE PARITY STATES OF NUCLEI IN THE A = 135 AND A - 190 MASS REGION

Author
Meyer-ter-Vetm, J.

Publication Date
1975

Submitted to Nuclear Physics A

LBL-3459
Preprint c.2

COLLECTIVE MODEL DESCRIPTION OF TRANSITIONAL ODD-A NUCLEI
II. COMPARISON WITH UNIQUE PARITY STATES OF NUCLEI IN THE A = 135 AND A = 190 MASS REGION

J. Meyer-ter-Vehn

January 1975

Prepared for the U. S. Atomic Energy Commission
under Contract W-7405-ENG-48

COLLECTIVE MODEL DESCRIPTION OF TRANSITIONAL ODD-A NUCLEI*

II. COMPARISON WITH UNIQUE PARITY STATES OF NUCLEI IN THE A = 135 AND A = 190 MASS REGION

J. Meyer-ter-Vehn†

Lawrence Berkeley Laboratory
University of California
Berkeley, California 94720

*Work performed under the auspices of the U. S. Atomic Energy Commission and supported in part by the Deutsche Forschungsgemeinschaft.

†On leave of absence from Physik-Department, Technische Universität München, München, West Germany

ABSTRACT

Recent experimental data on unique parity spectra of odd-A nuclei in the $A = 135$ and $A = 190$ mass region are compared in a systematic way with calculated energies and transition probabilities of a quasiparticle coupled to a rotating *triaxial* core. The comparison yields detailed evidence for triaxial shapes. Complex spectra of strongly-coupled structure as well as decoupled structure and various intermediate types are almost completely reproduced by the model with core parameters β and γ determined from neighboring even nuclei. The coexistence of $\Delta I = 2$ and $\Delta I = 1$ bandstructures, seen in some of the experimental spectra, is explained as a consequence of the shape asymmetry. In the $A = 190$ region, the odd-A spectra confirm the existence of a gradual shape transition from prolate-type shapes (^{186}Os, $\gamma = 16°$) to oblate-type shapes (^{198}Hg, $\gamma = 37°$). Energies and lifetimes in $A \approx 135$ nuclei reveal prolate triaxial shapes with γ-values in the range $20° < \gamma < 30°$. Contrary to the expectation of very γ-soft, fluctuating shapes which is based on calculated collective potentials, the present work seems to indicate that a number of transitional nuclei have rather stable triaxial shapes.

1. SOME GENERAL REMARKS

This is the second part of a collective model study on odd-A transitional nuclei. In Part I,[1]) the model of a single-j quasiparticle coupled to a rotating triaxial core has been investigated. A general survey about the calculated energies, moments, and transition probabilities has been given there including a physical interpretation of the results. In this second part, a systematic comparison of the model calculation with unique-parity states of transitional odd-A nuclei in the $A = 190$ and $A = 135$ mass region is presented. In general, the free parameters of the model, β, γ, and λ_F, are determined from neighboring even nuclei and from a single-particle level scheme. The details of this procedure are described in Section 2. The theoretical spectra, compared with experiment in Section 3, represent essentially parameter-free calculations.

It should be emphasized from the beginning that the assumption of rigid triaxial shapes with fixed values for β and γ is considered as an approximation to the actual nuclear wavefunctions. Against the general belief -- and also unexpected for the author of the present work -- this assumption turns out to be a very useful approximation which is well supported by new data most of them obtained from heavy-ion experiments during the last three years. They give new support to the old Davydov model and seem to indicate that a number of transitional nuclei have triaxial shapes which are considerably more stable than expected from theoretical potential-energy surfaces. This point will be discussed in Section 4.

In order to limit the size of this paper, no attempt is made to compare the calculated results with spectra of lighter nuclei and with normal-parity states also. The situation is more complex for normal-parity states since there are usually several j-shells of the same parity near the Fermi energy which tend to mix with each other. A systematic comparison with a mixed j-shell calculation will be interesting, but has not been performed so far.

2. DETERMINATION OF THE STANDARD PARAMETERS

In comparing the model calculation with experimental odd-A spectra, the goal is to determine the deformation parameter β and the asymmetry parameter γ from the lowest excited states of the adjacent even nuclei and to determine the Fermi energy λ_F from a single-particle level scheme. *No* parameter is then adjusted to the odd-A spectrum itself. Such a procedure is not completely unambiguous for several reasons:

(i) The low-energy spectra of even transitional nuclei differ in general from those of a perfect triaxial rotor, and there are different ways to adjust β and γ.

(ii) In a number of cases, the first excited energies of the even nuclei are rapidly changing with mass number so that the question arises which of the two neighbors or which average of them should be taken.

(iii) Furthermore, there is evidence in some cases that the odd nucleon polarizes the core so that the parameters of the even neighbors are not quite applicable to the odd-A nucleus.

Being aware of these ambiguities, a certain compromise has been chosen.

<u>The parameter γ</u> is determined from the energy ratio of the second 2^+ state to the nearest member of the groundstate band, in most cases

the first 4^+ state. For particle spectra (λ_F below j-shell), the (A-1) neighbor is chosen as reference nucleus and, for hole spectra (λ_F above the j-shell), the (A+1) neighbor. This procedure is well supported by the comparison with experiment. It can possibly be justified by stating that an odd-A spectrum should be compared with that even nucleus which has the same number of unbroken particle (or hole) pairs counting from the next closed shell. The energy ratios $E_{2_1^+}/E_{2_2^+}$, $E_{4_1^+}/E_{2_2^+}$, and $E_{6_1^+}/E_{2_2^+}$ are listed in Table 1 for different γ-values over the range $10° \leqslant \gamma \leqslant 30°$. Since the energy spectrum of the even triaxial rotor is symmetric about $\gamma = 30°$, this procedure cannot distinguish between prolate triaxial shapes $0° < \gamma < 30°$ and oblate triaxial shapes $30° < \gamma < 60°$. The information to which side a certain nucleus belongs has to be taken from the odd-A spectrum.

The parameter β is determined from the average $\bar{E}_{2^+} = \left(E_{2^+}^{(A-1)} + E_{2^+}^{(A+1)}\right)/2$ of the first 2^+ energies of the (A-1) and the (A+1) neighbor. Taking averages at this point seems to be inconsistent with the determination of γ; empirically, however, it yields the best overall agreement with experiment. Equating the expression

$$E_{2^+}^{th}(\gamma) = \frac{6\hbar^2}{2\mathcal{J}_o} \cdot \frac{9 - \sqrt{81 - 72\sin^2(3\gamma)}}{4\sin^2(3\gamma)}$$

for the first 2^+ energy of the even triaxial rotor with the experimental $\bar{E}_{2^+}$ and using the general relation $\hbar^2/(2\mathcal{J}_o) = 204\,\text{MeV}/(\beta^2 \cdot A^{7/3})$ (see Part I), one obtains

$$\beta = \left[\frac{1224}{A^{7/3} \cdot \bar{E}_{2^+}} \cdot X(\gamma) \right]^{\frac{1}{2}} ,$$

where $\bar{E}_{2^+}$ is taken in units MeV. The γ-dependent factor

$$X(\gamma) = E^{th}_{2^+}(\gamma) / (6\hbar/2\mathcal{J}_o)$$

is listed for convenience in column 5 of Table 1 for different γ.

The position of the Fermi energy λ_F relative to the j-shell on which the unique parity states are built determines the particle or the hole character of the spectrum. For a given j-shell, λ_F is estimated from a Nilsson level scheme for $\gamma = 0°$, since a good general level scheme showing the single-particle energies as functions of β *and* γ has not been at our disposal.† This estimate is sufficient as long as λ_F is

†Single-particle energies for $\beta = 0.3$ and $0° \leqslant \gamma \leqslant 60°$ are given in ref. [43]), for $0 < \beta < 0.6$ and $\gamma = 30°$ in ref. [31]).

located outside the j-shell level system. In cases where λ_F penetrates the j-shell appreciably, the fine adjustment of λ_F has been performed by fitting approximately the first $(j-1)$ state of the odd-A spectrum. In figs. 2 - 9, λ_F is given in the form $\tilde{\lambda}_F = (\lambda_F - \varepsilon_1)/(\varepsilon_2 - \varepsilon_1)$ for particle spectra and $\tilde{\lambda}_F = \left(\varepsilon_{(j+\frac{1}{2})} - \lambda_F\right)/\left(\varepsilon_{(j+\frac{1}{2})} - \varepsilon_{(j-\frac{1}{2})}\right)$ for hole spectra, where ε_ν with $\nu = 1,2,\ldots j+\frac{1}{2}$ are the single particle energies of the j-shell.

The parameters determined according to this procedure are called standard parameters. In the following comparison with experimental spectra, standard parameters are used unless stated differently.

3. COMPARISON WITH EXPERIMENT

3.1. The A = 190 Mass Region

Considerable evidence for triaxial shapes is found from odd-A nuclei in the A = 190 mass region. The experimental systematics of odd-proton negative-parity states are summarized in fig. 1. The energy spectra represent either particle states built on the $h_{9/2}$ shell or hole states built on the $h_{11/2}$ shell. For comparison, lowest excited states of the even nuclei in this region and their parameters β and γ are also given in fig. 1. One finds a remarkable constancy of the parameters as a function of neutron number (less pronounced for Os isotopes), however a strong variation with proton number as it approaches Z = 82. The standard parameters vary from $\beta = 0.23$ and $\gamma = 16°$ for ^{186}Os to $\beta = 0.13$ and $\gamma = 38°$ for the Hg isotopes. The γ-values of the heavier Pt isotopes are almost $\gamma = 30°$, but it is unclear whether slightly below or slightly above this value.

The variation of γ from shapes of prolate type ($0° < \gamma < 30°$) to shapes of oblate type ($30° < \gamma < 60°$) covers the interesting region where the theoretical odd-A spectra change from a decoupled level sequence (j, j-2, j+2, j+1, ...) to a strongly coupled level sequence (j, j+1, j+2, ...) for particle cases and vice versa for hole cases (compare fig. 6 and section 3.2. of Part I.) The theoretical expectation is nicely borne out by the experimental spectra, provided one associates the particle spectra with the (A - 1) even neighbor as core and the hole spectra with the (A + 1) even neighbor. Doing this, one expects, e.g., for ^{187}Ir, a decoupled $h_{9/2}$ spectrum on the $\gamma = 16°$ core of ^{186}Os, but at the same time a strongly coupled $h_{11/2}$ spectrum built on a hole in the $\gamma = 24°$ core of ^{188}Pt. For ^{189}Au, the prolate type ^{188}Pt now serves as a core for the $h_{9/2}$ spectrum, but the $h_{11/2}$ spectrum is built on the oblate type ^{190}Hg with $\gamma \approx 38°$, and both spectra are expected to be of decoupled structure in good agreement with experiment. One can follow this line one step further to the Tl isotopes where now the $h_{9/2}$ particle spectra on the oblate type Hg cores are of strongly coupled structure as expected. Note the remarkable constancy of the $h_{11/2}$ spectra in Au and the $h_{9/2}$ spectra in Tl for all isotopes which reflects the constancy of the Hg core energies. This survey already indicates that there is a continuous transition from the prolate side to the oblate side through the triaxial region. It can be followed over a series of nuclei. There is no sudden switch from $\gamma = 0°$ to $\gamma = 60°$.

The characteristics of the different triaxial regions can be traced to much finer details of the experimental data as will be shown in the following for some representative nuclei. Examples are picked out for which the measured data are most complete and which cover the range from ^{199}Tl to ^{187}Ir. Most evidence for triaxial shapes is obtained from the positions of unfavored yrast states and second and third states of the same spin, some of which form $\Delta I = 1$ bands beside the yrast band. These side bands are expected for triaxial odd-A rotors and will be discussed in connection with ^{187}Ir.

At the present time, there are much less data known for odd-neutron nuclei[14,15]) than for odd-proton nuclei. In the following collection, ^{193}Hg [15]) is included as one example for an $i_{13/2}$ neutron spectrum. Also the experimental results on moments and transition probabilities are still rare, but the few data known, e.g., for ^{187}Ir, agree well with the model calculation. The largest systematic discrepancy observed in the following examples concerns a general overall compression of the experimental spectra as compared with the calculated ones. This compression is equally observed for the neighboring even nuclei and reflects a certain softness of the actual wavefunctions which is not taken into account in the present rigid-rotor description.

3.1.1. ^{199}Tl

The negative-parity states of Tl isotopes[12]) represent a strong case for the present model. The strongly coupled bands built on the $h_{9/2}$ proton shell closely follow the spectrum of a rigid triaxial odd-A rotor. This is shown for ^{199}Tl in fig. 2. The theoretical spectrum is calculated with standard parameters except for β. A value $\beta = 0.15$, instead of $\beta = 0.13$ from ^{198}Hg or the even smaller value of ^{200}Pb, gives much improved agreement between the theoretical and the experimental spectrum. The larger β-value indicates that the $h_{9/2}$ particle has a deforming effect on the ^{198}Hg core.

Strong evidence for a triaxial shape is provided by the second $13/2^-$ state. As may be checked from fig. 6a in Part I, the energy of this state changes rapidly with γ relative to the groundband. Here, its experimental position is well reproduced with the standard value $\gamma = 37°$ derived from the ^{198}Hg core. Candidates for the $(13/2^-)_2$ state are also seen in ^{197}Tl and ^{195}Tl at about the same position. The 1943 keV state in ^{199}Tl can possibly be identified with the second $9/2^-$ model state. As does the $(13/2^-)_2$ state, it decays to the first $11/2^-$ state in the measured as well as in the calculated spectrum. The detection of the $5/2^-$ state should be a challenge for experiment. It is predicted to lie just below the $(13/2^-)_1$ state and should decay via E2 to the $(9/2^-)_1$ state or via E1 to the $3/2^+$ state at 367 keV in ^{199}Tl. The $(13/2^-)_2$ state has the character of a $(\overline{K} - \overline{\Omega} = +2)$ γ-band head built on the $9/2^-$ ground state (see section 3.4. and 3.5. of Part I). The $(9/2^-)_2$ state belongs to the corresponding low-spin band with $(\overline{K} - \overline{\Omega} = -2)$ character. It is interesting to note that the states of this band are most strongly decaying to the ground band rather than within the band. This band leaking will be further studied in examples that follow.

As seen in fig. 2, the decay within the groundband is not well reproduced by the calculation. This is probably due to an underestimate of the M1-transitions in the calculation; an effective $g_s \approx 0$ might be more appropriate for the $h_{9/2}$ system than the value $g_s = 0.6\, g_s^{free}$ used throughout this work. This is also indicated by the calculated magnetic moment $\mu = 2.9$ n.m. which is much smaller than the $h_{9/2}$ moments of about 4 to 5 n.m. measured in Re and Bi isotopes.[16]

3.1.2. ^{195}Au

The $h_{11/2}$ spectra in Au isotopes[10]) are based on the same oblate Hg cores as the $h_{9/2}$ systems in the Tl isotopes, but since they represent hole states they have a decoupled level order. In fig. 3, the standard model calculation is compared with the $h_{11/2}$ level scheme of ^{195}Au. The numerous high-spin and low-spin states known from heavy-ion and decay experiments are all reproduced by the model calculation including the transition branchings. Again, the result is rather specific concerning the shape asymmetry. For example, the near degeneracy of the first $9/2^-$ and $13/2^-$ states as well as the position of the unfavored $17/2^-$ yrast state just below the favored $19/2^-$ state and the near-crossing of the $(11/2^-)_2$ and $(11/2^-)_3$ states confine γ to within a few degrees about the standard Hg value $\gamma = 37°$. No comparable agreement would be obtained with an axially symmetric core.

Some finer details should be pointed out. As discussed in connection with fig. 5b in Part I, the second and third $11/2^-$ state exchange structure at a deformation $\beta \approx 0.15$, and one expects the transition probabilities in the decay of these states to vary strongly with β. In Table 2, relative transition intensities measured in ^{195}Au are compared with calculated ones. Fair agreement is obtained with a value $\beta = 0.144$ slightly larger than the standard value $\beta = 0.141$. The transition lines in fig. 5 are based on the calculation with $\beta = 0.144$. The very sharp change with β probably is a spurious result of the present model and would be smoothed by a more realistic wavefunction of the core.

Three more negative-parity states than shown in fig. 3 have been found for ^{195}Au in a recent decay study,[11]) a $9/2^-$ state at 1068 keV and two (9/2, 11/2, 13/2)$^-$ states at 1406 and 1487 keV. The calculation yields a second $9/2^-$ state, but no more $9/2^-$, $11/2^-$, or $13/2^-$ states in this region. Considering the decay of the additional states to their $9/2^-$ member and then most strongly to a $7/2^+$ state, one is tempted to attribute them to an $h_{9/2}$ system with a basic $9/2^-$ state and, depending thereon, an $11/2^-$ and a $13/2^-$ state, in analogy to the first $13/2^-$ and $15/2^-$ levels of the $h_{11/2}$ system. Provided this interpretation is right, the calculation accounts for all measured negative-parity states in ^{195}Au. The $h_{9/2}$ system has been observed beside the $h_{11/2}$ system in ^{189}Au,[7] ^{187}Ir,[2] and ^{189}Ir [2]. It can also be identified in ^{191}Au.[8]

3.1.3. ^{193}Hg

In fig. 4, the measured ^{193}Hg spectrum[15] (low-energy part < 1.5 MeV) built on an $i_{13/2}$ neutron hole is compared with the model calculation. The decoupled level order of the yrast band with the favored $13/2^+$, $17/2^+$, $21/2^+$, $25/2^+$ states and the unfavored $15/2^+$ and $19/2^+$ states is reproduced by both calculations for $\gamma = 38°$ and $\gamma = 60°$. This again confirms an oblate type shape for Hg isotopes. Evidence for triaxiality is given by the second 19/2 state which has been observed in experiment, though with an uncertainty concerning the parity. The relative independence on γ seen for *all* calculated yrast states is partly due to the Fermi energy which lies inside the $i_{13/2}$ shell for ^{193}Hg. There is a sharper variation of the unfavored states with γ, marking the triaxial region, in cases where λ_F is located outside the j-shell (see e.g., ^{195}Au in ref. 17).

3.1.4. ^{187}Ir ($h_{9/2}$ system)

Extensive data have been obtained recently for ^{187}Ir and ^{189}Ir.[2]

The spectra of the two nuclei look very similar. Beside positive-parity bands built on the $s_{1/2}$ and $d_{3/2}$ shell, two separate negative-parity families are observed and attributed to the $h_{9/2}$ and the $h_{11/2}$ shell. The $h_{9/2}$ system has a decoupled and the $h_{11/2}$ system a strongly coupled level order consistent with a prolate-type core. As seen in fig. 1, the adjacent even nuclei, e.g., of ^{187}Ir, possess quite different core parameters, for ^{186}Os, $\beta = 0.23$, and $\gamma = 16°$ and, for ^{188}Pt, $\beta = 0.18$ and $\gamma = 24°$. Comparing the ^{187}Ir data with the model calculation in figs. 5 and 6, good agreement is found when using the ^{186}Os parameters for the $h_{9/2}$ particle spectrum and the ^{188}Pt value $\gamma = 24°$ and an averaged $\beta = 0.21$ (standard procedure) for the $h_{11/2}$ hole spectrum. This result indicates that a kind of shape isomerism exists in ^{187}Ir and also in ^{189}Ir. It is also present in the Au isotopes.

In figs. 5 and 6, the calculated levels have been ordered according to the $(\overline{K},\overline{\Omega})$ classification discussed in Part I. Each column corresponds to an approximate $\overline{K}$ and $\overline{\Omega}$ value. The experimental states have tentatively been arranged in the same order on the basis of their energies and their decay transitions. An almost complete identification of the experimental levels seems to be possible within the present model. In particular, a number of unassigned levels can be understood as higher members of the $\Delta I = 1$ vertical band structure.

For the $h_{9/2}$ system, shown in fig. 5, a large number of favored and unfavored yrast states and 5 non-yrast states have been observed. Their relative order is almost completely reproduced by the calculation. The result again sensitively depends on the shape asymmetry and confirms the value $\gamma = 16°$ derived from the ^{186}Os core. The triaxial coupling scheme, discussed in Part I, classifies the favored yrast states as approximate $\overline{K} = \overline{\Omega}$, $\overline{\Omega} + 2$, $\overline{\Omega} + 4$, ... states with $\overline{\Omega} = 9/2$. On the low-spin side, the yrast is continued by approximate $\bar{K} = \bar{\Omega}-2$, $\bar{\Omega}-4$, $\bar{\Omega}-6$ states. Within the theoretical picture, the states on the yrast line mainly arise from collective rotation about the intrinsic $\hat{2}$-axis, whereas the states that build up on each yrast state are related to an additional rotation about the intrinsic $\hat{1}$-axis. The possibility of simultaneous rotation about two different intrinsic axes is a direct consequence of the triaxility of the core.

The vertical band structure is expected to exist only for a few lowest states. In the $h_{9/2}$ spectrum of ^{187}Ir, the states with relative energies 0 keV (9/2), 434 keV (11/2), 822 keV may be understood in this way as a $\bar{K} = \bar{\Omega} = 9/2$ band, and the states with energies 164 keV (13/2), 717 keV (15/2), 1135 keV as a $\bar{K} = \bar{\Omega} + 2 = 13/2$ band. The calculation suggests that higher states associated with this band structure predominantly decay to neighboring bands, in particular to yrast states. In fig. 5, this is seen for the $15/2^-$ model state at 1385 keV. Its strong decay to the $17/2^-$ and $13/2^-$ yrast states suggests that it corresponds to the measured 1061 keV state. On the basis of the triaxial model, one would therefore assign the experimental states at 822, 1061, and 1135 keV (relative energy) as second $13/2^-$, $15/2^-$, and $17/2^-$ states, respectively. There are more high-spin model states below 1.4 MeV, not shown in fig. 6: two $9/2^-$ states at 829 and 1070 keV, two $11/2^-$ states at 1082 and 1377 keV, and another $13/2^-$ state at 1306 keV. Their calculated decays, however, agree much less or not at all with the decay pattern of the unassigned experimental levels.

3.1.5. ^{187}Ir ($h_{11/2}$) system)

The $h_{11/2}$ spectrum of ^{187}Ir is compared with the calculation in fig. 6. Energies and transition probabilities of this spectrum and of corresponding levels in heavier Ir isotopes strongly support the triaxial model. An interpretation assuming an axially symmetric core must fail. On the one hand, the low-lying $7/2^-$ state and its strongly enhanced $B(E2;\ 7/2 \rightarrow 11/2) = 0.3\ (eb)^2$, measured for ^{189}Ir,[4]) could only be understood assuming an oblate core. On the other hand, the strongly coupled level order of the yrast band gives a clear indication for a prolate core. The suspicion of shape asymmetry has been raised in the past[6]) and is substantiated by the present work.

The triaxial model calculation, using standard parameters, yields a low-lying $7/2^-$ state with a calculated $B(E2;\ 7/2^- \rightarrow 11/2^-) = 0.32\ (eb)^2$ simultaneously with the strongly coupled yrast band. In addition, it reproduces and elucidates the fairly complex level structure seen beside the yrast band and tentatively identifies five unassigned experimental states. It also provides good agreement between calculated and measured B(E2)-branching ratios and mixing ratios which are compared in Tables 3a and 3b.

Some further comments should be made with respect to fig. 6. The bands of the calculated spectrum are classified from left to right as $(\overline{K} = 7/2,\ \overline{\Omega} = 11/2)$, $(\overline{K} = 5/2,\ \overline{\Omega} = 9/2)$, $(\overline{K} = \overline{\Omega} = 9/2)$, $(\overline{K} = \overline{\Omega} = 11/2)$, $(\overline{K} = 13/2,\ \overline{\Omega} = 9/2)$, and $(\overline{K} = 15/2,\ \overline{\Omega} = 11/2)$ bands. They are related to 11/2[505] and 9/2[514] Nilsson bands and the corresponding low- and high-spin γ-bands. One should keep in mind, however, that these bands are strongly mixed and that the $(\overline{K},\overline{\Omega})$ character is weakly defined in general (compare discussion in Part I). Though of rotational character, their band structure is often difficult to recognize experimentally since transitions within these bands are sometimes weaker than those to neighboring bands, in particular the yrast band. For example, the measured 1127 keV state decaying to the $15/2^-$ yrast state is likely to be the 15/2 member of the $\bar{K} = 13/2$ band both because of its energy and its decay. The classification of the measured 1287 keV state is unclear, though it might correspond to the $17/2^-$ state of the same band.

Although the general structure of the $h_{11/2}$ spectrum in ^{187}Ir can be understood assuming a fixed shape, there are some indications for parameter variations within this level system. For example, the staggering of the experimental yrast band, which is not reproduced by the standard calculation shown in fig. 6, would be obtained with slightly larger values for γ and λ_F. This can be checked, e.g., in fig. 8 where the $h_{11/2}$ spectrum of ^{137}Nd and the corresponding calculation is shown. As a second point, the calculation for ^{187}Ir yields the $7/2^-$ band too high relative to the $11/2^-$ band, indicating that the γ-value of the experimental $7/2^-$ band is slightly larger than that used in the calculation. The ^{187}Ir result suggests that the Pt core on which the $h_{11/2}$ spectrum in ^{187}Ir is based is more γ-soft than, e.g., the Hg cores on which the $h_{11/2}$ spectra in Au and the $h_{9/2}$ spectra on Tl are built.

3.2. The A = 135 Mass Region

In the region with $Z > 50$ and $N < 82$, which was discovered as a new region of deformation a decade ago,[18)] even nuclei consistently show a low-lying second 2^+ state at about the energy of the first 4^+ state. This suggests that shape asymmetry might be important. First excited 0^+ states appear well separated at higher energies and exclude a two phonon interpretation. Parameters β and γ of some even nuclei in this region are derived according to the standard procedure and are listed together with the lowest excitation energies in Table 4. Considerable variations of β with mass number are found, whereas the γ-values are fairly constant in the range $20^{\circ} < \gamma < 30^{\circ}$. Decoupled odd-A spectra built on $h_{11/2}$ proton particles as well as strongly coupled spectra built on $h_{11/2}$ neutron holes are observed in this mass region and clearly indicate prolate-type shapes. Oblate shapes have been assumed in the past[19,20]), but they are ruled out also by recent measurements of quadrupole moments in even Ba isotopes[21]).

The exciting point about odd-A spectra and, in particular, families of unique-parity states is that they give more information about the shapes than just a classification as prolate or oblate; they allow to determine the shape asymmetry rather sensitively. Although the available experimental material on odd-A nuclei in the A = 135 mass region is still less abundant than for A ≈ 190 nuclei, there already exists considerable evidence that the new region of deformation is mainly a triaxially deformed region -- at least around A = 135. This conclusion is based

(i) on $h_{11/2}$ proton spectra observed in ^{133}La, [22,23,24]) ^{135}La, [24]) ^{135}Pr, [25]) and ^{129}Cs, [24])

(ii) on yrast bands built on an $h_{11/2}$ neutron hole in ^{135,137}Nd, [26]) ^{133,135}Ce, [26]) and ^{131}Ba, [27]) and on the decay spectrum of ^{137}Pr to ^{137}Nd, [28]) and

(iii) on a recent lifetime measurement of favored yrast states in ^{129}La. [29])

Part of this evidence is discussed in the following. A lifetime measurement in ^{107}Cd, similar to that in ^{129}La, is included in the discussion because of its general interest.[30])

3.2.1. ^{135}Pr

The $h_{11/2}$ odd-proton spectra in the A = 135 mass region can be considered as the particle analogues of the $h_{11/2}$ hole spectra in the Au isotopes. For the Au isotopes, one has $\gamma \approx 37^o$, and the Fermi energy lies above the $h_{11/2}$ shell, $\lambda_F > \varepsilon_{11/2}$; for La and Pr isotopes, one has $\gamma \approx 23^o$ (= $60^o - 37^o$) and $\lambda_F < \varepsilon_{11/2}$. Due to the particle-hole symmetry (compare Part I), the corresponding $h_{11/2}$ spectra look very similar.

In fig. 7, this is demonstrated for ^{135}Pr, one of the rare cases in this region where both high-spin and low-spin data are available.[25]) Beside the standard triaxial calculation with $\gamma = 23^o$, the model solution for $\gamma = 0^o$ is also shown for comparison. The effect of the triaxiality of the core is most evident for the group of second and third states with spin $7/2^-$, $9/2^-$, $11/2^-$ just below the $19/2^-$ yrast state. Possible theoretical partners for the experimental states are found in this energy region in the triaxial calculation, but lie far too high in energy for an axially symmetric core. This strongly supports the assumption of shape asymmetry in ^{135}Pr. Concerning transition-branching ratios, experiment and theory do not compare well enough to identify these states separately.

The standard calculation yields more states in the region around the $19/2^-$ state: a $5/2^-$ state at 1279 keV, a $13/2^-$ state at 1456 keV, a $3/2^-$ state at 1517 keV, a $15/2^-$ state at 1700 keV, and a $17/2^-$ state at 1746 keV. Since the ^{135}Pr spectrum is fed by decay from a $9/2^-$ state in ^{135}Nd with all log (ft) values < 7, these states are probably not populated. The $5/2^-$ state has been observed near the expected energy in ^{133}La for which a spectrum similar to that of ^{135}Pr has been found.[23,24])

3.2.2. ^{129}La and ^{107}Cd

Another test for shape asymmetry in spectra with decoupled level order is based on lifetimes of the favored yrast states. Although the favored energies do not strongly depend on γ, the B(E2)-values do, as shown in fig. 9 of Part I. The calculated ratios $R = B(E2; (j+2) \rightarrow j)/B(E2; 2^+ \rightarrow 0^+)$ drop from values $R \approx 1.5$ for axially symmetric shapes at $\gamma = 0^o$ to values $R \approx 1.2$ for $\gamma = 20^o$ and $R \approx 0.9$ for $\gamma = 25^o$. The ratios R are also slightly dependent on β and λ_F.

A recent measurement[29]) for ^{129}La yields a preliminary value $B(E2; 15/2^- \rightarrow 11/2^-)/B(E2; 2^+ \rightarrow 0^+) = 1.15$ (± 10%) which indicates a $\gamma \approx 21^o$ in good agreement with the standard value $\gamma = 22^o$ of ^{130}Ba. No additional states of ^{129}La beside the yrast band are known at the moment to check this value with other odd-A data. A similar measurement has recently been reported for ^{107}Cd. [30]) In this case, the negative-parity states are based on an $h_{11/2}$ neutron particle. A value $B(E2; 15/2^- \rightarrow 11/2^-)/B(E2; 2^+ \rightarrow 0^+) = 1.16$ (± 5%) very similar to that of ^{129}La is obtained. The ^{107}Cd measurement is in excellent agreement with the triaxial rotor model which yields $R = 1.17$ taking $\gamma = 22^o$ from the energies and $\beta = 0.177$ from the B(E2)'s in $^{106,108}Cd$ and $\lambda_F = 0$ from the level scheme in ref.[31]). This is a very interesting result since ^{107}Cd has a rather small parameter $\beta \cdot A^{2/3} = 4.0$ and is expected to be at the border to the weak-coupling region. Neverthelesss, the ^{107}Cd result is well described in the present rotor model. In ref.[30]), it has been interpreted in terms of the particle-phonon model. Both models seem to reproduce the experimental value. A distinction between them might be possible based on B(E2)'s of higher yrast transitions.

3.2.3. ^{137}Nd

Combined data for ^{137}Nd, obtained from heavy-ion and β-decay experiments,[26,28] are compared with theory in fig. 8. With 77 neutrons ^{137}Nd is the neutron analogue of ^{187}Ir which has 77 protons. As seen from the comparison of fig. 6 and fig. 8, the $h_{11/2}$ spectra of both nuclei -- at least their high-spin part -- are remarkably similar. As in ^{187}Ir, a strongly coupled, heavily distorted yrast band is observed in ^{137}Nd and indicates a triaxial shape. It is well reproduced by the calculation with standard parameters and confirms γ to lie within a few degrees about the standard value $\gamma = 26°$, derived from ^{138}Nd. In fact, the staggering of the yrast band and the narrow spacing between the $(13/2^-)_1$ and $(15/2^-)_1$ states point to a slightly larger γ.

There is an additional group of negative-parity levels observed in ^{137}Nd as shown on the left-hand side of fig. 8. These levels should also be understandable within the model. One could think of the 1374 keV state as the $(7/2^-)_1$ model state, but, on this assumption, it should strongly decay to the basic $11/2^-$ state and not to the $(9/2^-)_1$ state as in experiment. The experimental level system built on the 1899 keV state is also difficult to understand within the $h_{11/2}$ model spectrum, since the potential partners among the model states in this region predominantly decay to the $\overline{K} = \overline{\Omega} = 9/2$ and $\overline{K} = \overline{\Omega} = 11/2$ bands and not to their next neighbors as in experiment. Our conclusion, therefore, is that these states are *not* based on the $h_{11/2}$ shell.

It would be tempting, however, to attribute the system on the 1899 keV state to the $h_{9/2}$ shell and possibly the states at 1374 keV and 1788 keV to the $f_{7/2}$ shell which should show up in this energy region and in this order. Provided this interpretation would be right, the states at 2370 keV, 2433 keV, 2722 keV, and 2804 keV could be attributed to $(11/2)_1$, $(13/2)_1$, $(13/2)_2$, and $(11/2)_2$ states, respectively, based on the $h_{9/2}$ state at 1899 keV. The corresponding calculation indicates a $\gamma \approx 30°$. All these states would be easily populated in the decay from the $11/2^-$ parent state in ^{137}Pr. Unfortunately, however, the expected $h_{9/2}$ (1899 keV) $\rightarrow$ $h_{11/2}$ (520 keV) transition has not been seen in experiment so that no definite conclusion can be drawn at the moment. For a systematic study, more experimental results in neighboring nuclei are needed.

3.2.4. ^{133}Ce

The N = 75 isotones ^{135}Nd, ^{133}Ce, and ^{131}Ba exhibit almost identical negative parity spectra.[26,27] The case ^{133}Ce is presented in fig. 9. Again, the experimental spectrum is much better reproduced by the standard triaxial calculation than by the $\gamma = 0°$ solution. A discrepancy, however, remains for the lowest 9/2 state. Although the penetration of the Fermi energy into the $h_{11/2}$ shell brings the 9/2 state down, it is not lowered far enough. This difficulty with $I < j$ states is known from Coriolis distorted bands in strongly deformed nuclei and is usually remedied by an ad hoc attenuation of the Coriolis matrix elements. No such procedure has been adopted in this work, since it would obscure the clear physical outlines of the present model. A physical explanation of this effect has been given recently by Ring and Mang,[32] based on a self-consistent treatment of the core moment-of-inertia. It is still an open question how to incorporate their treatment into a triaxial-rotor model where one has three rotation axes rather than one.

4. DISCUSSION OF RESULTS AND RELATIONS TO OTHER MODELS

It has been shown that the predictions of the triaxial-rotor-plus-quasiparticle model are in remarkable agreement with a number of unique-parity spectra of odd-A transitional nuclei. It describes the nucleus ^{199}Tl at the border to the closed-shell Pb region as well as ^{187}Ir which borders strongly deformed rare-earth nuclei. It also seems to apply to the $50 < Z$, $N < 82$ nuclei though more experimental data are needed to confirm its validity in that region. How is this success of a rigid triaxial rotor model to be interpreted? It would be naive to take the rigid shape literally. There is much evidence that these transitional nuclei have fairly soft fluctuating shapes. The question is rather *to which extent* these nuclei are soft or rigid and what one can learn about it from the present result. In what follows, a qualitative answer is given.

Assuming that the collective motion of low-excited nuclei is dominated by the quadrupole degrees of freedom, the nuclear softness is most conveniently discussed in terms of potential-energy surfaces (PES) in the (β,γ) plane. Figure 10 displays some typical situations in a schematic way:

1) Fig. 10a: The harmonic-vibrator PES which only occurs for closed shell nuclei and their next neighbors.

2) Fig. 10b: The prolate-rotor PES with a deep potential minimum at $\beta_o \neq 0$ and $\gamma_o = 0$ which is characteristic for well deformed nuclei.

3) Fig. 10c: The γ-soft PES which has a relative maximum at $\beta = 0$ and shows a shallow valley at $\beta_o \neq 0$ with the deeper minimum either at $\gamma = 0°$ (prolate type) or at $\gamma = 60°$ (oblate type).

4) Fig. 10d: The triaxial-rotor PES which is similar to the γ-soft PES but possesses a clear minimum in the triaxial region.

The existing microscopic calculations of PES in the $A = 190$ and $A = 135$ mass region consistently yield PES of the γ-soft type without any pronounced triaxial minima.[33,34,35,36] This result seems to be inconsistent with the present result as well as with empirical data of even-A nuclei. The evidence from even nuclei is discussed first.

(i) A specific test for complete γ-softness is the simultaneous degeneracy of the 2_2^+ and 4_1^+ states and the 3_1^+ and 4_2^+ states of the quasi-γ-band. This double degeneracy occurs for a completely γ-independent PES *no matter* what the β-dependence is (model of Wilets and Jean[37]). In Table 5, data for ^{190}Os and ^{124}Xe which have $E_{2_2^+} \cong E_{4_1^+}$ are compared with the γ-soft case and the triaxial rotor. It is seen that the measured γ-band ratios are inconsistent with complete γ-softness which, on the other hand, has been obtained approximately from microscopic calculations for ^{190}Os and ^{124}Xe. Also the rigid-triaxial-rotor limit is not reached, indicating that the actual wavefunctions are neither sharply localized nor equally distributed in the γ-valley, but have a certain limited spread -- for ^{190}Os less than for ^{124}Xe. Such wavefunctions would be obtained from the triaxial type of PES shown in fig. 10d.

(ii) A similar result has been obtained by Gneuss and Greiner[38] and more recently by Habs et al.[39] based on a fit of the anharmonic-vibrator model to low-energy data. These empirical PES of nuclei in the $A = 135$ region show pronounced minima of triaxial type in disagreement with microscopically calculated PES.

The result of the present work on odd-A nuclei points into the same direction. The question is to which extent the odd particle is able to shift the average parameters of the core. The odd-A energies vary strongly as functions of γ, and, for a very γ-soft potential, one would expect large variations of γ within a family of odd-A states and also in comparison with the even neighbors. A feeling for this effect can be obtained from results of Kumar and Baranger on even nuclei in the A=190 mass region. Based on calculated PES and a dynamic treatment of β and γ, they derive rms-values of β and γ for the lowest excited states. Some results for ^{186}Os and ^{196}Pt are given in Table 6. In the groundstate band, γ_{rms} moves slightly towards $\gamma=0^{\circ}$ for ^{186}Os and towards $\gamma=60^{\circ}$ for ^{196}Pt with increasing energies; for the second 2^{+} state, however, it is sharply pushed towards $\gamma=30^{\circ}$. This is just what one expects from the slopes of the triaxial-rotor energies as functions of γ (compare fig. 2, Part I) in the case of γ-soft shapes. Since the energy of the 2_2^{+} state comes down steeply for $\gamma \rightarrow 30^{\circ}$, it tends to push the core in this direction.

In contrast to these theoretical results, the present comparison with experimental odd-A spectra indicates that the γ-deformations are rather stable. E.g. for the odd-A Au-isotopes, our result is definitely in disagreement with large variations of γ comparable to those of γ_{rms} shown in Table 6. One could think of a stabilisation due to the odd particle; but this would not explain why the h11/2 spectrum in Au and the h9/2 spectrum in Tl consistently lead to the same $\gamma=37^{\circ}$, within $\pm 2^{\circ}$ or so, as the Hg cores. Our conclusion is therefore that the Hg cores themselves are less γ-soft than calculated PES in this mass region and that they have probably triaxial potential minima of the kind shown in fig. 10d. A similar conclusion seems to be indicated by the present work for Os, Pt, and even-A cores around A=135, although the present evidence for these cases is not as strong as for the Hg-isotopes.

One would like to make the conclusion more quantitative. This would require, however, a calculation, similar to that of Gneuss and Greiner, for odd-A nuclei in which the odd particle is coupled to a parameterized anharmonic vibrator or at least a γ-soft vibrator (only β fixed!) and in which the parameters are fitted to experiment. This procedure would make more sense for the odd-A case than for the even-A case since there are much more data known in the low-energy region for odd-A nuclei which would check the model. Unfortunately, no results of such calculations are at our disposal at the moment.

In the past, odd-A transitional nuclei have been described on a spherical basis coupling a quasiparticle to one or two phonons. Such calculations have been performed on a large scale by Kisslinger and Sorensen who used RPA phonons based on the pairing-plus-quadrupole model[40]). Most published results are given for low-lying normal-parity states, and no comparison with the present results on unique-parity states is possible.

Interesting calculations have been performed recently by Paar within the Alaga model[41]) for nuclei which are three particles or three holes away from closed shells. In these calculations, three particle (hole)-clusters are coupled to one and two phonons of closed-shell nuclei. Anharmonicities are considered to arise exclusively from the particle-phonon coupling. It will be interesting to compare the results of the triaxial-rotor model with those of the Alaga model, e.g., for Au isotopes, when they become available.

5. CONCLUSION

Stimulated by new results from heavy-ion and β-decay experiments, families of unique-parity states in transitional odd-A nuclei have been investigated in a systematic way. Although quite different types of level orders are observed in these spectra, they all appear to arise from the same physical structure. This structure can be described in a relatively simple and intuitive model consisting of an odd nucleon coupled to a triaxial rotating core.

In the best experimental cases, e.g., in ^{187}Ir and ^{195}Au, 13 or more states of one family are known at low energy ($< 2\Delta$). The model calculation reproduces *all* states in almost the right order, including high-spin *and* low-spin states. The unique-parity systems have been studied here for nuclei in the $A = 190$ and $A = 135$ mass region. Similar spectra, however, have also been seen in some lighter nuclei, and they possibly represent a general structure characteristic for weakly deformed open-shell nuclei.

The model depends only on the three parameters, β, γ, and λ_F, which have a direct physical significance and can be determined almost independently from the odd-A spectra. As a function of the deformation parameter $\beta \cdot A^{2/3}$, the model describes different strengths of core-particle coupling intermediate between weak coupling and strong coupling, whereas the variations with γ provide the main clue for understanding the variety of different level orders observed in experiment. A most beautiful example for these changes is given by the unique-parity spectra in Ir, Au, and Tl isotopes. The gradual shape transition in this mass region from strongly deformed prolate to weakly deformed oblate shapes through a series of triaxial shapes is reflected in detail by these spectra in agreement with the present theoretical description.

The puzzling result of this work is that the odd-A spectra define γ rather sharply, within ± 2° or so for cases like ^{195}Au or ^{137}Nd, and that, within this margin, these values coincide consistently with those derived from the even neighbors -- the (A - 1) neighbor for particle and the (A + 1) neighbor for hole spectra. This result is at variance with the expectation of very γ-soft shapes which are predicted by calculated potential-energy surfaces for these transitional nuclei. An odd-A calculation based on a dynamic treatment of β and γ is strongly suggested by the present result to check, in particular, the influence of γ-softness on the odd-A spectra quantitatively. Due to the large number of levels at low energy, the construction of empirical collective potentials from odd-A spectra should make more sense than corresponding attempts from even nuclei. Based on the present work, one expects potentials with rather pronounced minima in the triaxial region. If this expectation can be confirmed, it will have serious implications for the calculated collective potentials which, so far, do not show such minima.

The present work has strong applications in the field of experiment. It provides a general frame for analyzing low-energy spectra of transitional odd-A nuclei. It predicts numerous states, their energies, moments, and transition probabilities, which have not yet been measured. More experimental results are necessary to judge the range of validity of the present model. Certain discrepancies are expected due to shape fluctuations and other effects. But the present work clearly points out that there is a simple general structure behind the intricate and, so far, poorly understood odd-A spectra in the transitional regions and that the concept of triaxial nuclear deformations represents a natural way to understand their systematic behavior.

ACKNOWLEDGMENTS

The author thanks Dr. J. Jastrzebski for the communication of unpublished data on ^{187}Ir of the Grenoble-Swierk collaboration and the permission to use them in this publication. He thanks Dr. R. M. Diamond and Dr. F. S. Stephens for their great help concerning this work and acknowledges helpful discussions with Prof. J. Rasmussen, Dr. N. Glendenning, and Dr. W. J. Swiatecki, Dr. C. Gerschel, Dr. J. Gizon, Dr. D. Habs, Dr. R. A. Meyer, and Dr. C. Sebille-Schück. He also thanks Dr. E. Browne and Dr. R. Doebler from the Table-of-Isotopes group for critical comments on experimental data and thanks Dr. N. Glendenning for the hospitality of the Nuclear Theory group in Berkeley.

REFERENCES

1) J. Meyer-ter-Vehn, Nucl. Phys. (Part I of this work).

2) Grenoble-Swierk collaboration; S. André, J. Boutet, J. Rivier, J. Treherne, J. Jastrzebski, J. Lukasiak, Z. Sujkowski, and C. Sebille-Schück, Proc. Int. Conf. on Reactions between Complex Nuclei, (Nashville, 1974), Eds. R. L. Robinson et al., Vol. I (North-Holland, Amsterdam, 1974), p. 192, and submitted to Nucl. Phys.

3) C. Sebille-Schück, M. Finger, R. Foucher, J. P. Husson, J. Jastrzebski, V. Berg, S. G. Malmskog, G. Astner, B. R. Erdal, P. Patzelt, and P. Siffert, Nucl. Phys. A212 (1973) 45.

4) A. Bäcklin, G. Hedin, and S. G. Malmskog, Nucl. Phys. A156 (1970) 647.

5) A. Bäcklin, G. Hedin, and S. G. Malmskog, Nucl. Phys. A169 (1971) 122.

6) R. H. Price, D. G. Burke, and M. W. Johns, Nucl. Phys. A176 (1971) 338.

7) V. Berg, M. A. Deleplanque, C. Gerschel, and N. Perrin, IPNO-Ph.N-74-12, Inst. Phys. Nucl., BP. no. 1-91406 (Orsay, France).

8) H. Beuscher, P. Jahn, R. M. Lieder, and C. Mayer-Böricke, Z. Physik 247 (1971) 383.

9) M. B. Lewis and M. J. Martin, Nucl. Data Sheets 8 (1972) 389 and 431.

10) P. O. Tjøm, M. Maier, D. Benson, Jr., F. S. Stephens, and R. M. Diamond, Nucl. Phys. A231 (1974) 397.

11) Ch. Vieu, A. Peghaire, and J. S. Dionisio, Revue de Physique Appliquée 8 (1973) 231.

12) J. O. Newton, S. D. Cirilov, F. S. Stephens, and R. M. Diamond, Nucl. Phys. A148 (1970) 593, and to be published.

[13]) M. Sakai, Institute for Nuclear Study report INS-J-142(1973),University of Tokyo, Tokyo (Japan).

[14]) D. Proetel, D. Benson, Jr., A. Gizon, J. Gizon, M. R. Maier, R. M. Diamond, and F. S. Stephens, Nucl. Phys. A226 (1974) 237.

[15]) H. Beuscher, W. F. Davidson, R. M. Lieder, A. Neskaskis, and C. Mayer-Böricke, Phys. Rev. Letters 32 (1974) 843.

[16]) V. S. Shirley, in Hyperfine Interactions in Excited Nuclei, Editors G. Goldring and R. Kalish, Vol. IV (Gordon & Breach, New York, 1971) p. 1255.

[17]) J. Meyer-ter-Vehn, F. S. Stephens, and R. M. Diamond, Phys. Rev. Letters 32 (1974) 1383.

[18]) R. K. Sheline, T. Sikkeland, and R. N. Chanda, Phys. Rev. Letters 7 (1961) 446.

[19]) K. Kumar and M. Baranger, Phys. Rev. Letters 12 (1964) 73.

[20]) C. W. Towsley, R. Cook, D. Cline, and R. N. Horoshko, J. Phys. Soc. Japan, Vol. 34 (Suppl.) (1973) 442.

[21]) J. J. Simpson, D. Eccleshall, M. J. L. Yates and N. J. Freeman, Nucl. Phys. A94 (1967) 177;
R. Kerns and J. X. Saladin, Phys. Rev. C6 (1972) 1016;
M. Neiman, R. Kalish, D. R. S. Somayajulu, B. Herskind, F. Genovese, and L. Grodzins, Phys. Letters 52B (1974) 189.

[22]) J. R. Leigh, K. Nakai, K. H. Maier, F. Pühlhofer, F. S. Stephens, and R. M. Diamond, Nucl. Phys. A213 (1973) 1.

[23]) E. A. Henry and R. A. Meyer, Lawrence Livermore Laboratory report UCRL-75676 (1974), Livermore (USA).

[24] R. Hayano, J. Chiba, M. Sekimoto, H. Nakayama, and K. Nakai, University of Tokyo preprint (1974), Tokyo (Japan).

[25] J. van Klinken, D. Habs, H. Klewe-Nebenius, K. Wisshak, G. P. Nowicki, J. Buschmann, S. Göring, R. Löhken, H. Rebel, and G. Schatz, Ges. f. Kernforschung report KFK-1768 (1974), Karlsruhe (West Germany).

[26] J. Gizon, A. Gizon, M. R. Maier, R. M. Diamond, and F. S. Stephens Nucl. Phys. A222 (1974) 557.

[27] J. Gizon, A. Gizon, and D. J. Horen, Proceedings International Conf. on Reactions between Complex Nuclei, Nashville, 1974, Editors R. L. Robinson et al., Vol. I (North-Holland, Amsterdam, 1974), p. 154.

[28] G. P. Nowicki, Ges. f. Kernforschung report KFK-2017 (1974), Karlsruhe (West Germany).

[29] D. Ward, private communication.

[30] O. Häusser, D. J. Donahue, R. L. Hershberger, R. Lutter, F. Ries, H. Bohn, T. Faestermann, F. V. Feilitzsch, and K. E. G. Löbner, Phys. Letters 52B (1974) 329.

[31] A. Faessler, J. E. Galonska, U. Goetz, and H. C. Pauli, Nucl. Phys. A230 (1974) 302.

[32] P. Ring and H. J. Mang, Phys. Rev. Letters 33 (1974) 1174.

[33] K. Kumar and M. Baranger, Nucl. Phys. 110 (1968) 529, and Nucl. Phys. A122 (1968) 273.

[34] D. A. Arseniev, A. Sobiczewski, and V. G. Soloviev, Nucl. Phys. A126 (1969) 15.

[35] U. Goetz, H. C. Pauli, K. Alder, and K. Junker, Nucl. Phys. A192 (1972) 1.

36) I. Ragnarsson, A. Sobiczewski, R. K. Sheline, S. E. Larsson, and B. Nerlo-Pomorska, Nucl. Phys. A233 (1974) 329.

37) L. Wilets and M. Jean, Phys. Rev. 102 (1956) 788.

38) G. Gneuss and W. Greiner, Nucl. Phys. A171 (1971) 449.

39) D. Habs, H. Klewe-Nebenius, K. Wisshak, R. Löhken, G. Nowicki, and H. Rebel, Z. Physik 267 (1974) 149.

40) L. S. Kisslinger and R. A. Sorensen, Rev. Mod. Phys. 35 (1963) 853.

41) V. Paar, Nucl. Phys. A211 (1973) 29.

42) M. Sakai, Institute for Nuclear Study report INS-J-146 (1974), University of Tokyo, Tokyo (Japan).

43) U. Goetz, H. C. Pauli, and K. Alder, Nucl. Phys. A175 (1971) 481.

Table 1. Ratios of the first 2_1^+, 4_1^+, and 6_1^+ energies to the second 2_2^+ energy for a triaxial rotor with irrotational moments-of-inertia.

γ	$E_{2_1^+}/E_{2_2^+}$	$E_{4_1^+}/E_{2_2^+}$	$E_{6_1^+}/E_{2_2^+}$	$E_{2_1^+}/\left(\frac{6\hbar^2}{2\mathcal{J}_0}\right)$
10°	0.062	0.208	0.434	1.06
11°	0.076	0.253	0.527	1.08
12°	0.092	0.305	0.632	1.09
13°	0.108	0.357	0.738	1.11
14°	0.126	0.415	0.854	1.13
15°	0.146	0.476	0.973	1.15
16°	0.167	0.543	1.10	1.17
17°	0.186	0.603	1.25	1.19
18°	0.214	0.685	1.40	1.21
19°	0.239	0.758	1.54	1.24
20°	0.267	0.838	1.60	1.27
21°	0.296	0.910	1.73	1.30
22°	0.326	0.982	1.86	1.33
23°	0.327	1.05	1.98	1.36
24°	0.387	1.12	2.11	1.39
25°	0.417	1.18	2.22	1.42
26°	0.445	1.23	2.32	1.45
27°	0.466	1.27	2.39	1.47
28°	0.482	1.30	2.44	1.48
29°	0.495	1.32	2.48	1.49
30°	0.500	1.33	2.50	1.50

Table 2. Experimental and theoretical relative transition rates in the decay of the second and third $11/2^-$ state of ^{195}Au. Experimental energies relative to the first $11/2^-$ state identify the states.

I_i	E_i [keV]	→	I_f	E_f [keV]	Relative Transition Rates: $Exp^{a)}$	Theory $\beta = 0.144$	Theory $\beta = 0.141$
11/2	962	→	9/2	575	1	1	1
			13/2	560	0.06	0.16	0.37
			7/2	207	0.20	0.39	6.26
			11/2	0	0.65	0.57	4.17
11/2	1028	→	9/2	575	0.69	0.87	1.38
			13/2	560	1	1	1
			7/2	207	--	0.03	0.09
			11/2	0	0.36	0.79	0.78

[a] Ref. [9].

Table 3a. Comparison of experimental and theoretical B(E2)-branching ratios within the $h_{11/2}$ system of ^{187}Ir.

Transitions	B(E2)-ratios Exp[a]	Theory
$\frac{(15/2)_1 \rightarrow (11/2)_1}{(15/2)_1 \rightarrow (13/2)_1}$	$1.7^{+\infty}_{-1.4}$	5.5
$\frac{(17/2)_1 \rightarrow (13/2)_1}{(17/2)_1 \rightarrow (15/2)_1}$	$0.8^{+0.2}_{-0.6}$	0.8
$\frac{(15/2)_2 \rightarrow (11/2)_1}{(15/2)_2 \rightarrow (13/2)_1}$	< 0.1	0.02
$\frac{(19/2)_1 \rightarrow (15/2)_1}{(19/2)_1 \rightarrow (15/2)_2}$	$1.3^{+3.1}_{-0.6}$	1.4

[a] Ref. [2]).

Table 3b. Comparison of experimental and theoretical mixing ratios $\delta(E2/M1)$ within the $h_{11/2}$ system of ^{187}Ir. Measured transition energies have been used for calculating $\delta(E2/M1)$.

Transition	E_γ [keV]	$\delta(E2/M1)$ Exp[a]	$\delta(E2/M1)$ Theory
$(15/2)_1 \rightarrow (13/2)_1$	200	$0.0 < \delta < 0.25$	0.06
$(13/2)_1 \rightarrow (11/2)_1$	330	$0.25 < \delta < 0.40$	0.22
$(17/2)_1 \rightarrow (15/2)_1$	389	$0.15 < \delta < 0.25$	0.23
$(15/2)_2 \rightarrow (13/2)_1$	395	$0.28 < \delta$	0.25
$((9/2)_1 \rightarrow (11/2)_1$	385	$-0.40 < \delta < -0.15$	-0.08

[a] Ref. [2]).

Table 4. Lowest excitation energies in the A = 135 mass region[13]) and derived parameters.

Isotope	Z	N	$E_{2_1^+}$	$E_{4_1^+}$	$E_{2_2^+}$	β	γ	$\beta \cdot A^{2/3}$
Xe^{128}	54	74	443	1033	970	0.213	23°	5.4
Xe^{130}	54	76	536	1204	1122	0.190	23°	4.9
Xe^{132}	54	78	668	1440	1298	0.169	24°	4.4
Ba^{130}	56	74	357	902	908	0.231	22°	5.9
Ba^{132}	56	76	465	1128	1032	0.203	24°	5.3
Ba^{134}	56	78	605	1401	1168	0.177	25°	4.6
Ce^{132}	58	74	325	858	--	0.240	--	6.2
Ce^{134}	58	76	409	1049	966	0.210	23°	5.5
Ce^{136}	58	78	553	1316	1093	0.182	25°	4.8
Nd^{134}	60	74	294	789	--	0.256	--	6.7
Nd^{136}	60	76	374	974	--	0.223	--	5.9
Nd^{138}	60	78	521	1250	1014	0.185	26°	4.9

Table 5. Comparison of theoretical and experimental energy ratios of the the quasi-γ-band.

	Theory		Experiment	
	γ-soft	Triaxial rotor ($\gamma = 22.2°$)	^{190}Os [a]	^{124}Xe [b]
$E_{2_2^+} / E_{4_1^+}$	1	1	1.02	0.96
$\frac{E_{4_2^+} - E_{2_2^+}}{E_{3_1^+} - E_{2_2^+}}$	1	2.73	2.01	1.47

[a] Ref. [13].
[b] Ref. [42].

* * * * *

Table 6. Comparison between calculated β_{rms} and γ_{rms} values and standard β and γ fit-values of this work.

	^{186}Os Kumar, Baranger [a]		^{186}Os this work		^{196}Pt Kumar, Baranger [a]		^{196}Hg this work	
	β_{rms}	γ_{rms}	β	γ	β_{rms}	γ_{rms}	β	γ
0_1^+	0.223	23.2°	0.23	16°	0.154	36.2°	0.13	37°
2_1^+	0.230	21.1°			0.168	38.9°		
4_1^+	0.239	19.6°			0.181	40.5°		
2_2^+	0.226	33.4°			0.173	31.2°		

[a] Ref. [33].

FIGURE CAPTIONS

Fig. 1. Systematics of unique-parity spectra built on the $h_{9/2}$ and the $h_{11/2}$ shell of odd-proton nuclei in the A = 190 mass region. Energies (in keV) of adjacent even nuclei and standard values for β and γ or estimates (in brackets) are given.[13]) Spin values (2I) and positions of odd-A states are based on: ^{187}Ir ref. 2, 3; ^{189}Ir ref. 2, 4; ^{191,193}Ir ref. 5, 6; ^{189}Au ref. 7; ^{191}Au ref. 8 and systematics; ^{193}Au ref. 9; ^{195}Au ref. 9, 10, 11; Tl isotopes ref. 12.

Fig. 2. Negative-parity states in ^{199}Tl. Solid lines indicate the strongest observed and calculated decay transitions of each level.

Fig. 3. Negative-parity states in ^{195}Au. Energies are given in keV relative to the $11/2^-$ state at 318 keV. Solid lines indicate transitions with 80 to 100%, broken lines transitions with 20 to 80% of the strongest decay intensity of each level. Calculated intensities are based on calculated B(E2)- and B(M1)-values, but experimental transition energies when known.

Fig. 4. Positive-parity states in ^{193}Hg.

Fig. 5. The $h_{9/2}$ family of negative-parity states in ^{187}Ir. Energies are given in keV relative to the $9/2^-$ state at 186 keV. Calculated transition lines are defined as in fig. 3; experimental ones are solid for the strongest transition and broken for weaker transitions.

Fig. 6. The $h_{11/2}$ family of negative-parity states in ^{187}Ir. The calculated quadrupole moment and magnetic moment for the basic $11/2^-$ state are given. For more details see fig. 5.

Fig. 7. Negative-parity states in ^{135}Pr below the $19/2^-$ state. The second $9/2^-$ and the third $11/2^-$ state, calculated for $\gamma = 0°$, lie at higher energies (given in keV) than shown.

Fig. 8. Negative-parity states in ^{137}Nd. The definition of the transition lines is given in fig. 3. Not all theoretical transitions are shown.

Fig. 9. Negative-parity states in ^{133}Ce.

Fig. 10. Schematic potential-energy surfaces for different types of nuclei.

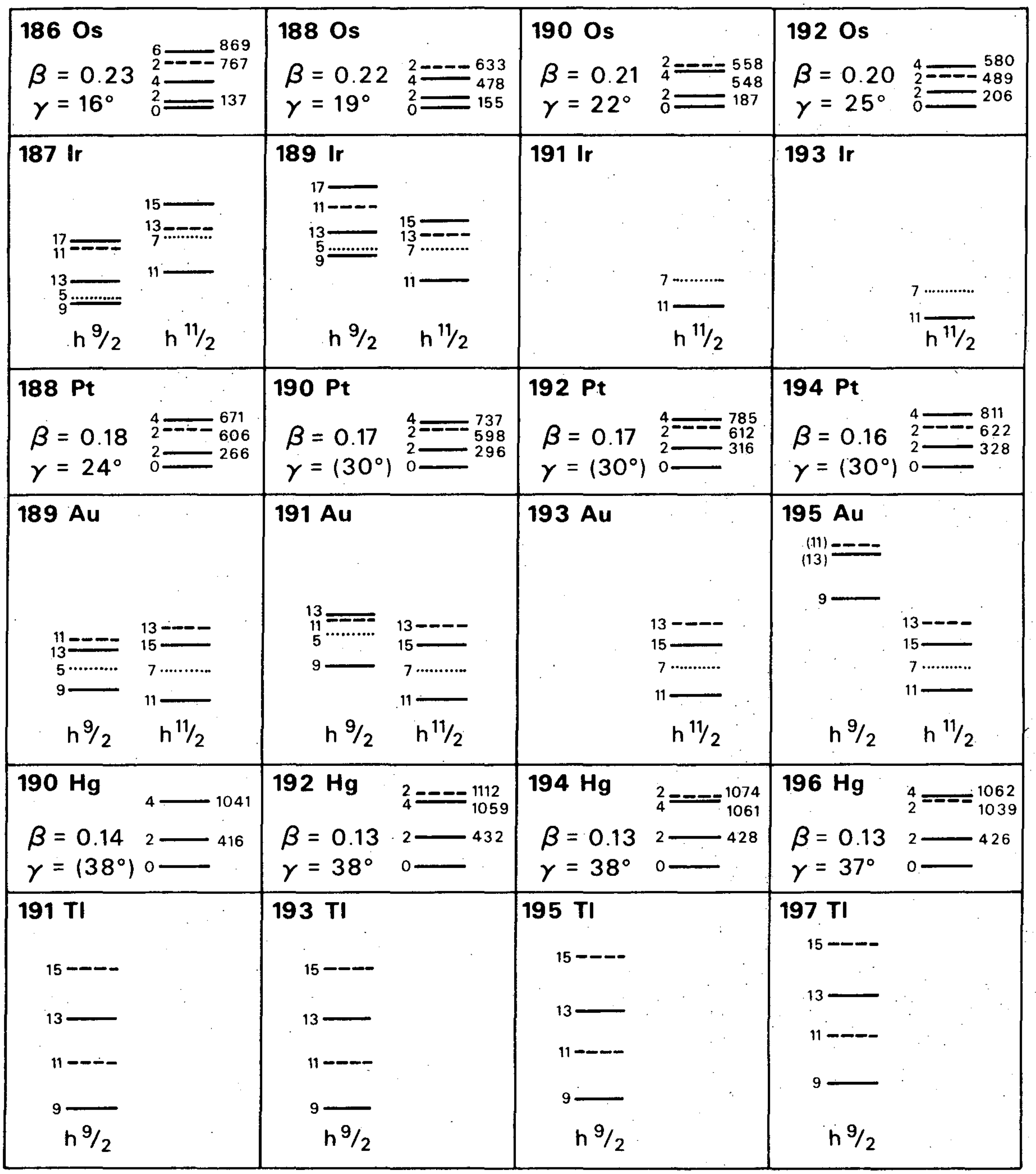

XBL 7411-8166

Fig. 1

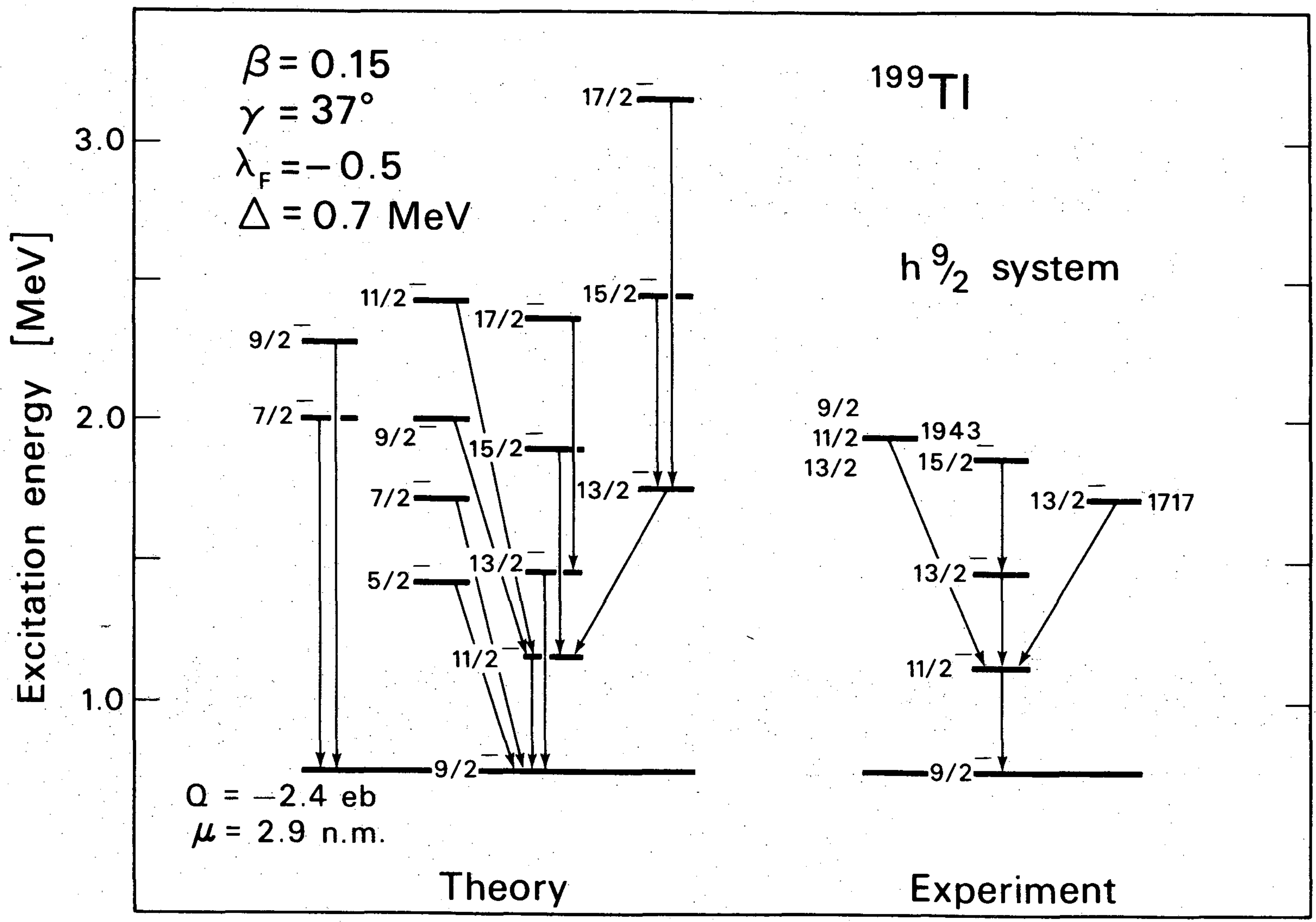

XBL 7411-8170

Fig. 2

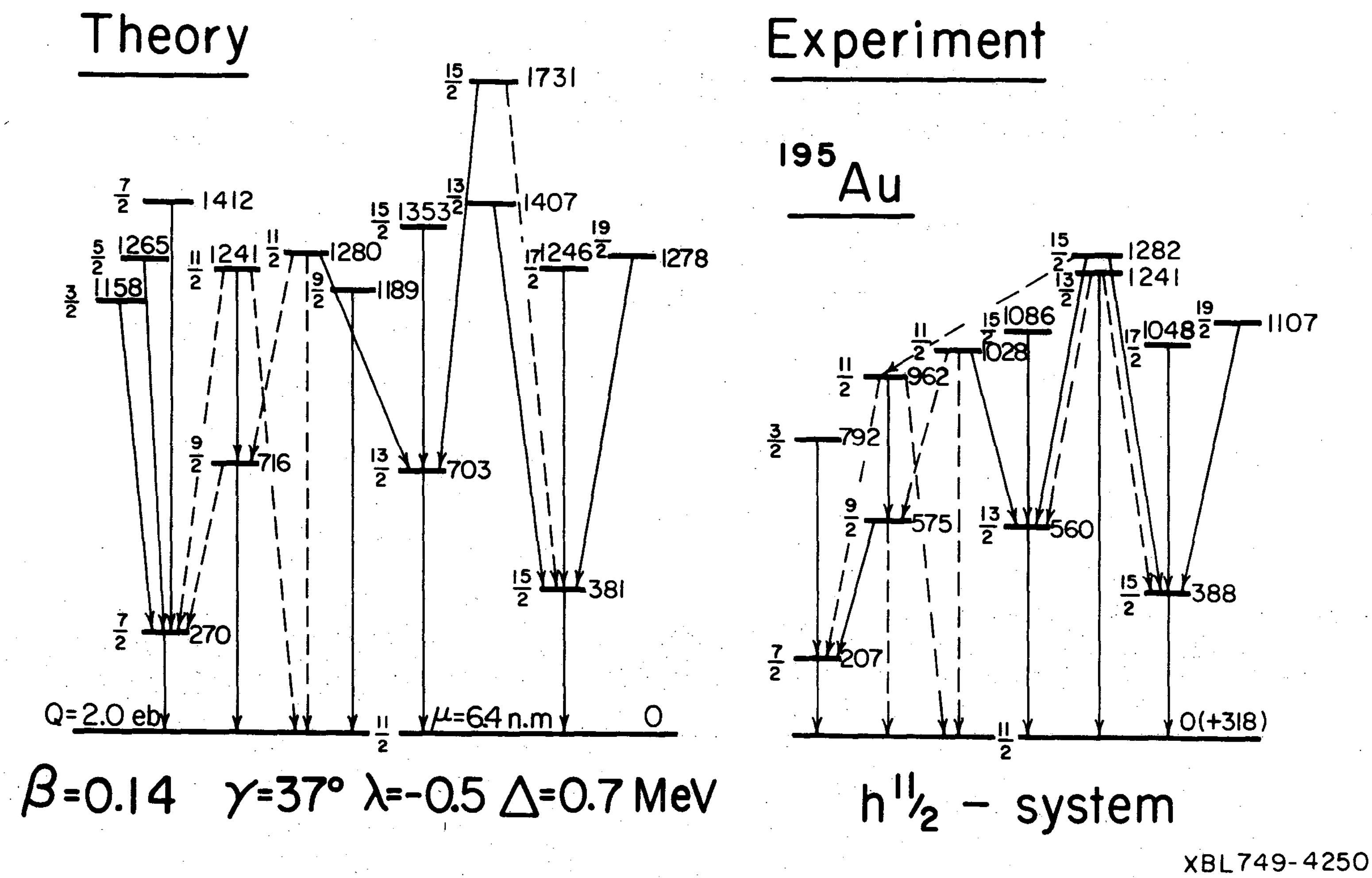

Theory
Experiment
195 Au
Q=2.0 eb
μ=6.4 n.m
0
0(+318)
β=0.14 γ=37° λ=-0.5 Δ=0.7 MeV
h11/2 - system
XBL749-4250

Fig. 3

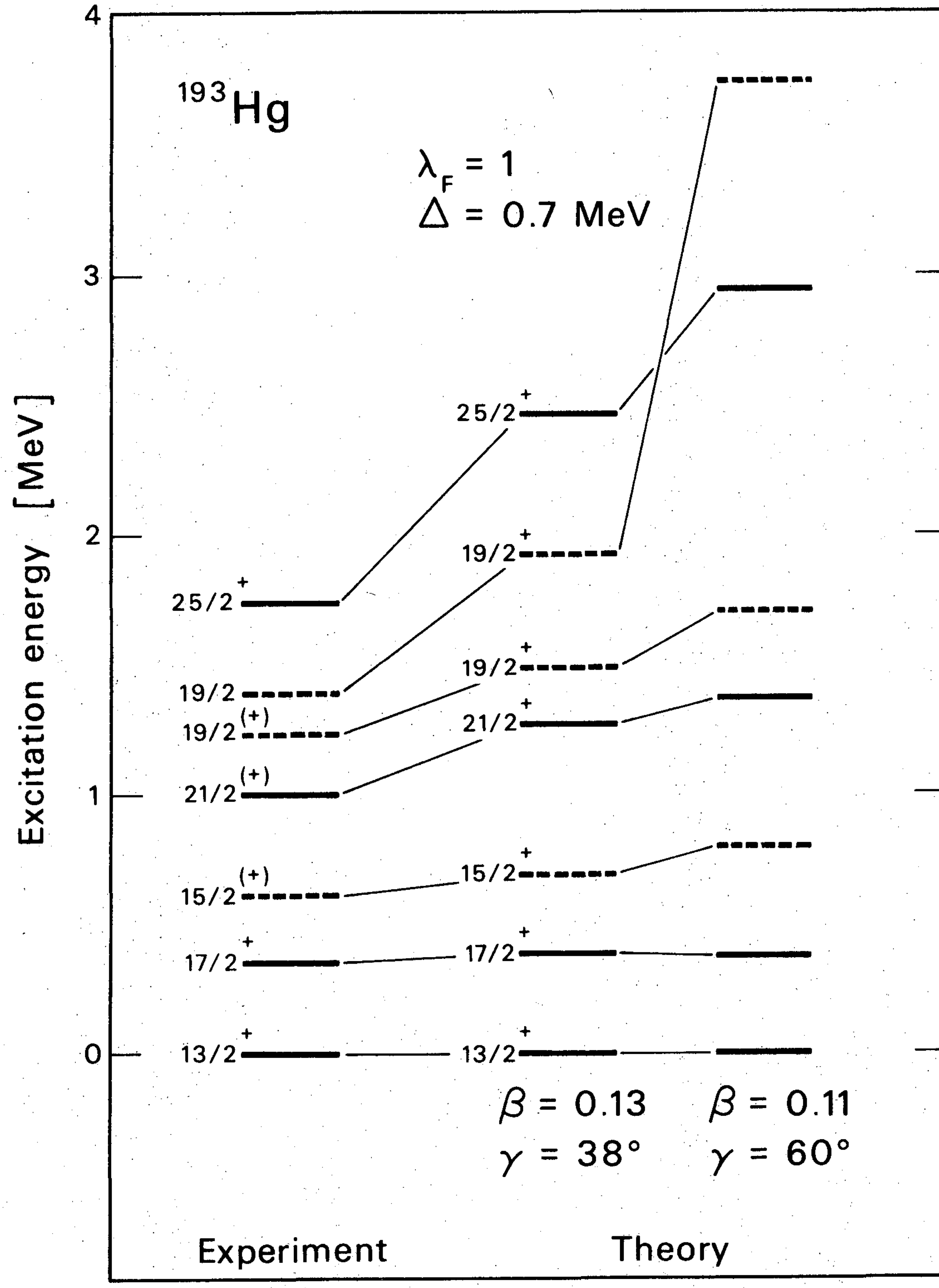

XBL 7411-8171

Fig. 4

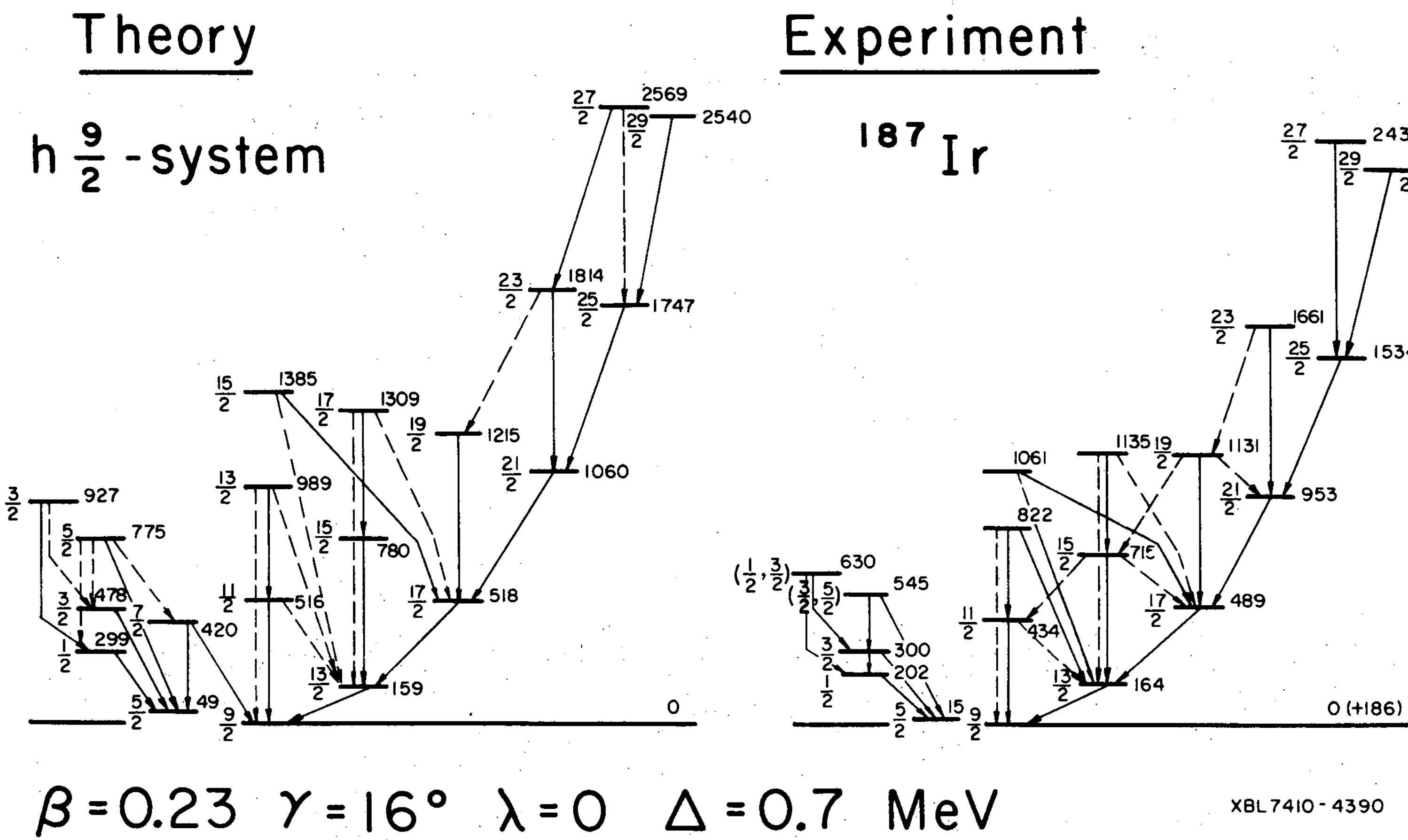
Theory
Experiment
h 9/2 -system
187 Ir
β = 0.23 γ = 16° λ = 0 Δ = 0.7 MeV
XBL 7410 - 4390

Fig. 5

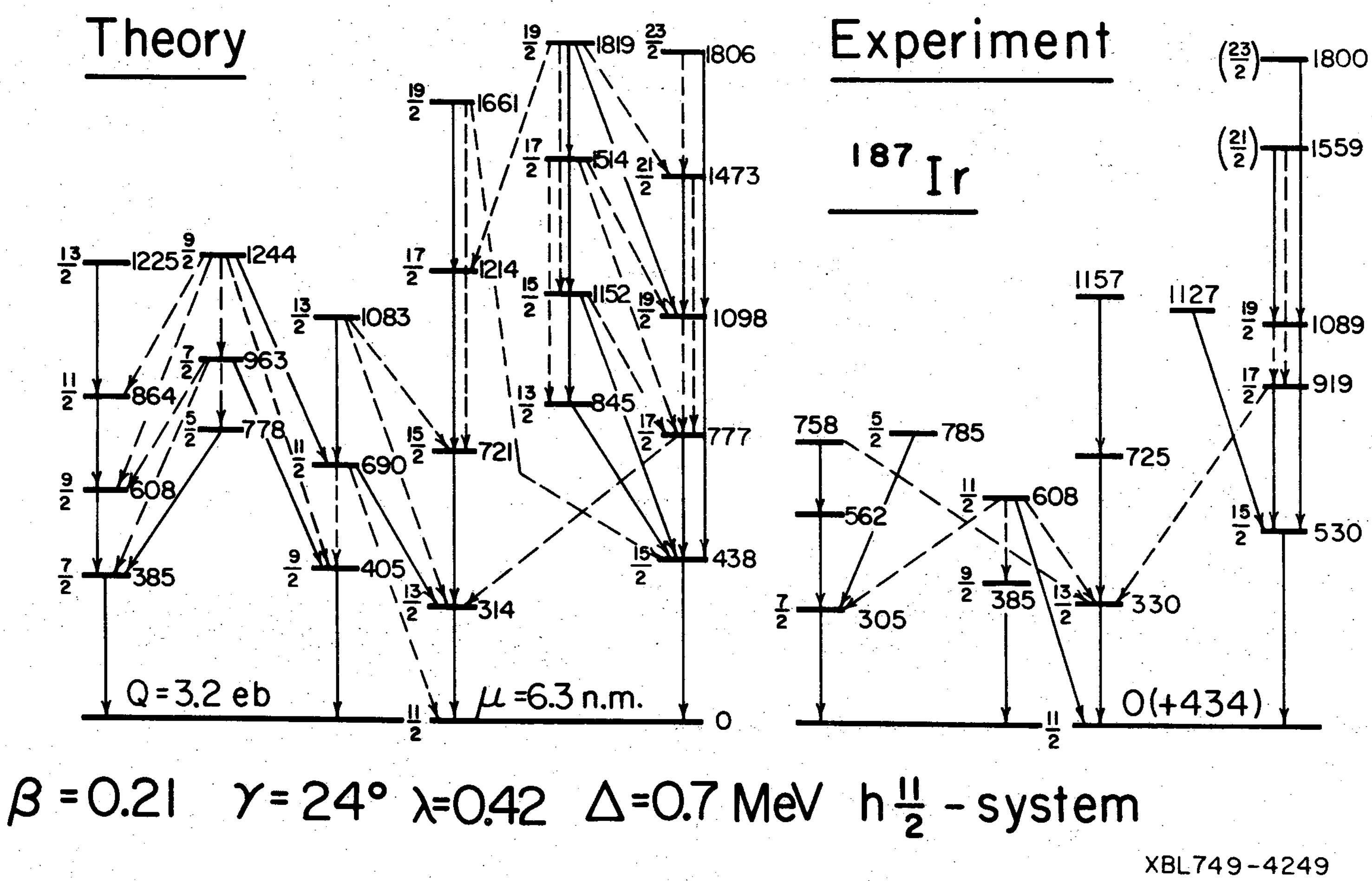

Theory
Experiment
187 Ir
Q = 3.2 eb
μ = 6.3 n.m.
0(+434)
β = 0.21 γ = 24° λ = 0.42 Δ = 0.7 MeV h 11/2 - system
XBL749-4249

Fig. 6

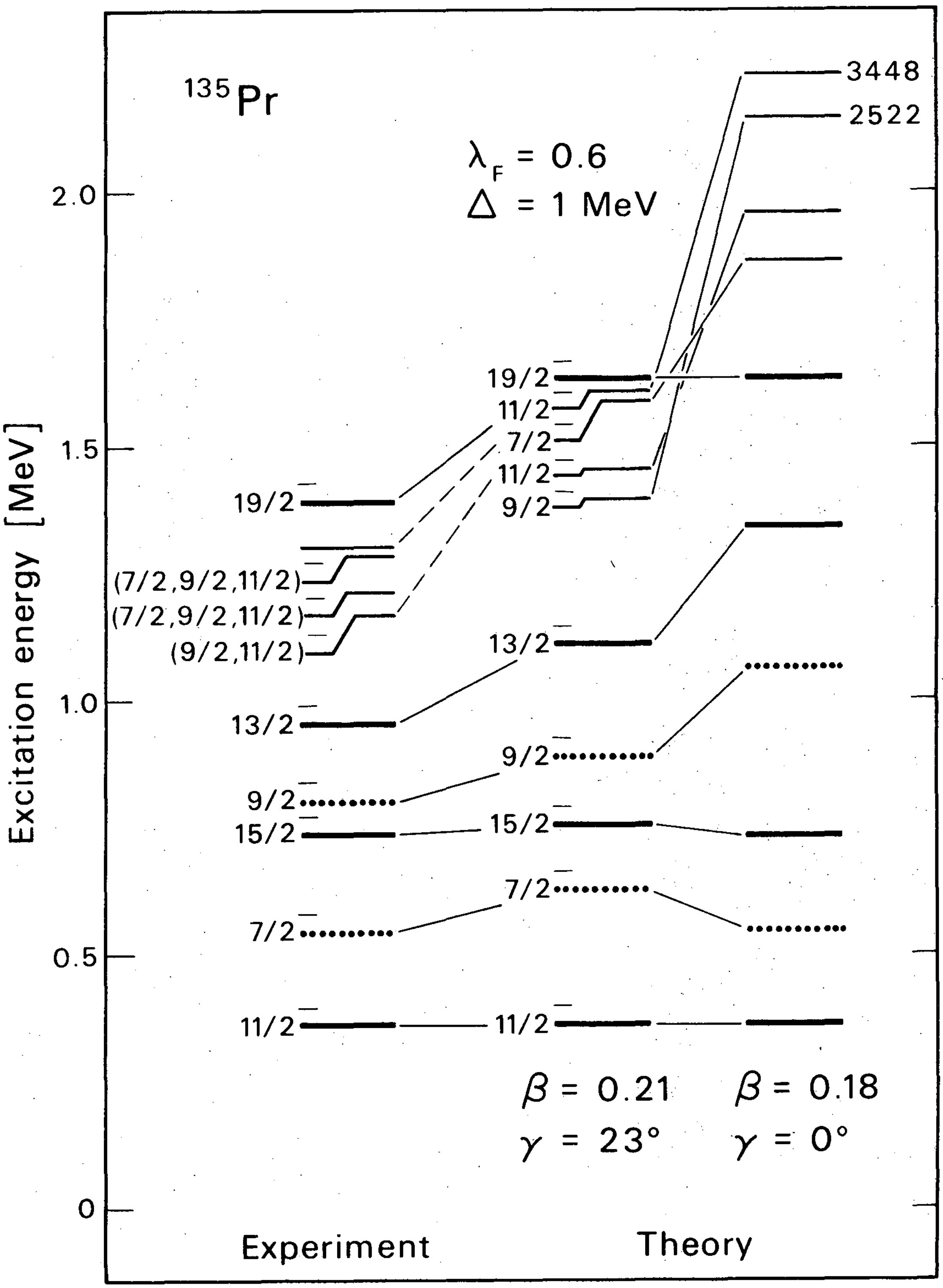

XBL 7412-8175

Fig. 7

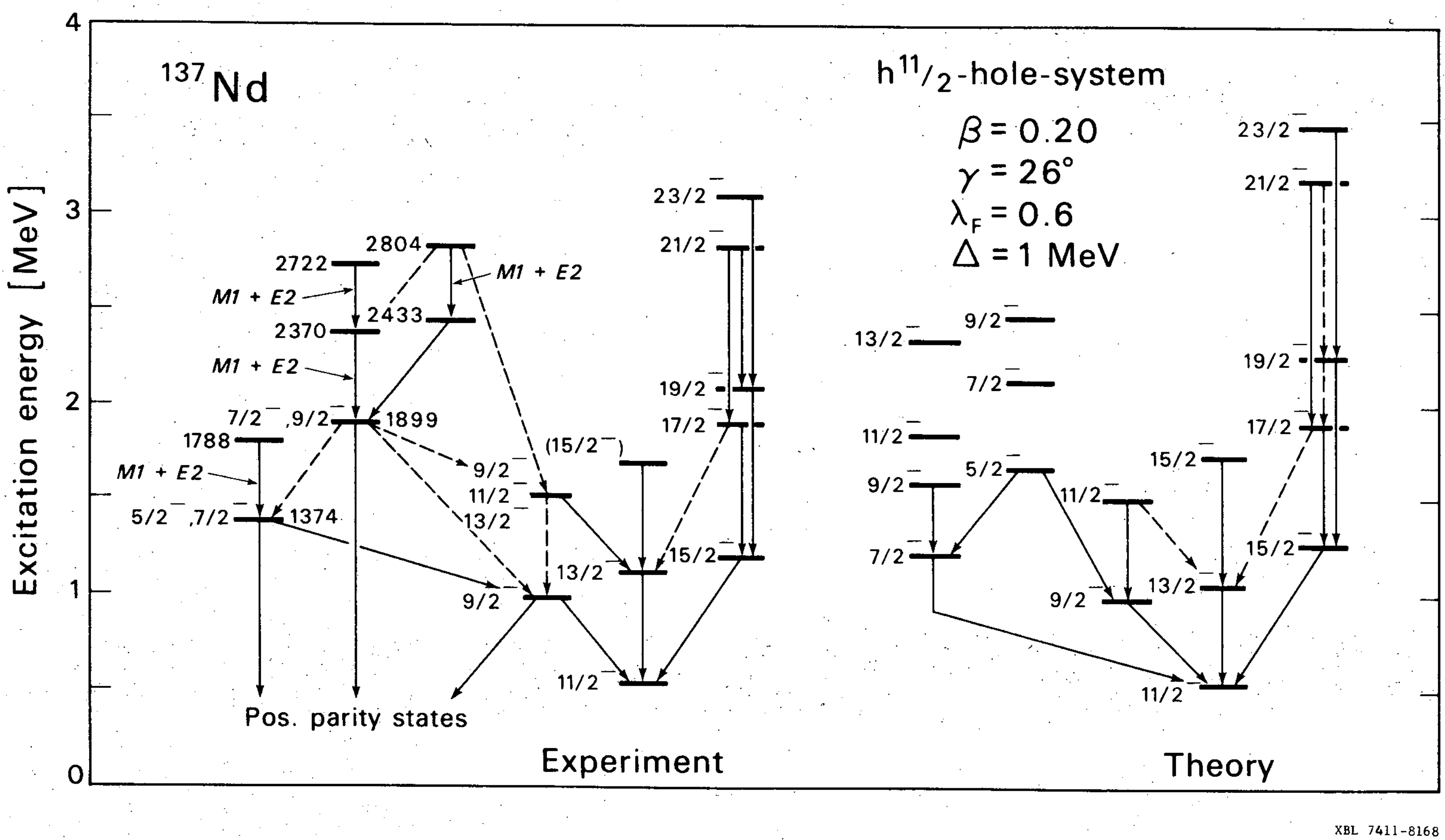

137Nd
h11/2-hole-system
β = 0.20
γ = 26°
λF = 0.6
Δ = 1 MeV
Excitation energy [MeV]
2804
2722
M1 + E2
2433
2370
7/2−, 9/2− 1899
1788
5/2−, 7/2− 1374
Pos. parity states
9/2−
11/2−
13/2−
(15/2−)
23/2−
21/2−
19/2−
17/2−
15/2−
Experiment
Theory
XBL 7411-8168

Fig. 8

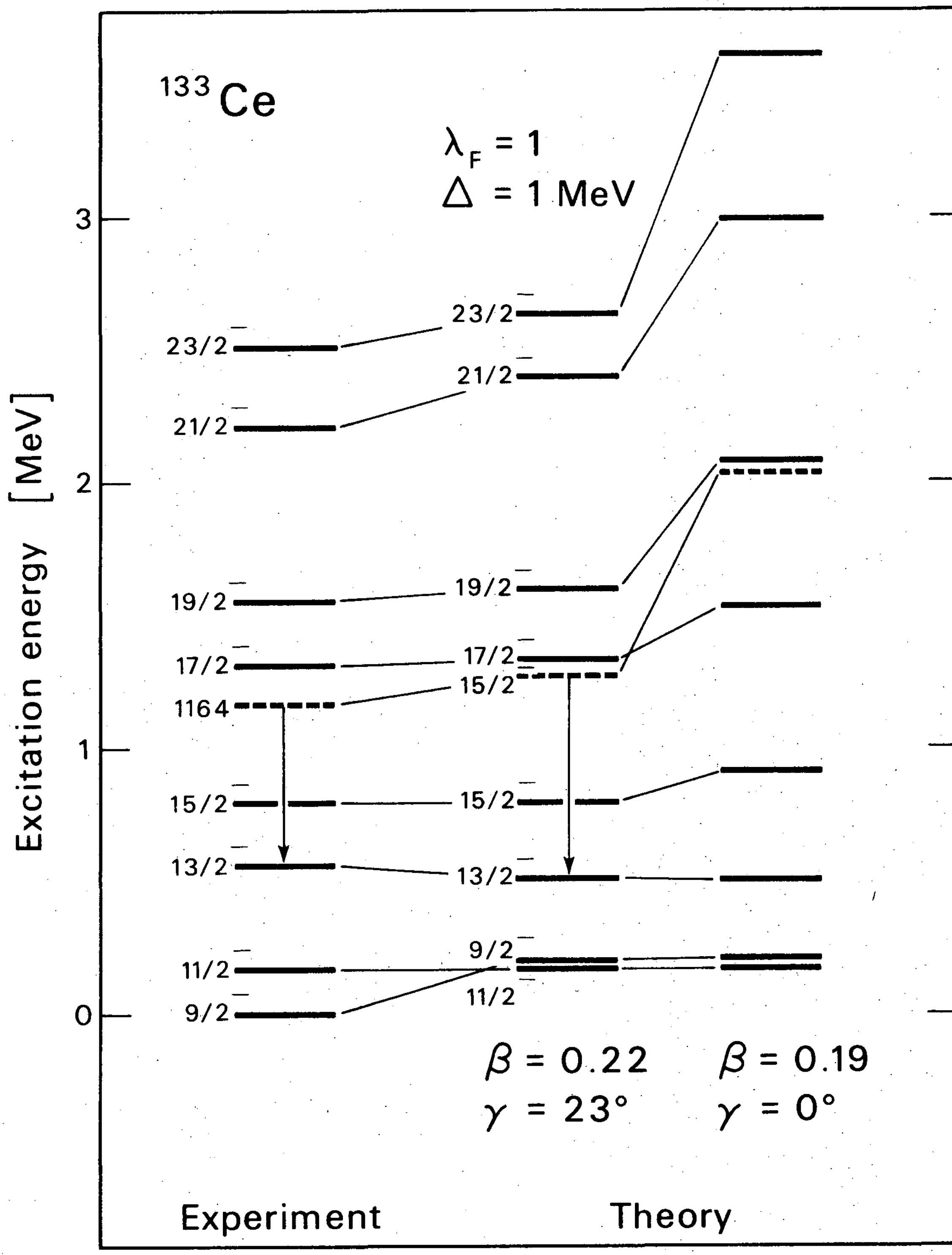

XBL 7411-8172

Fig. 9

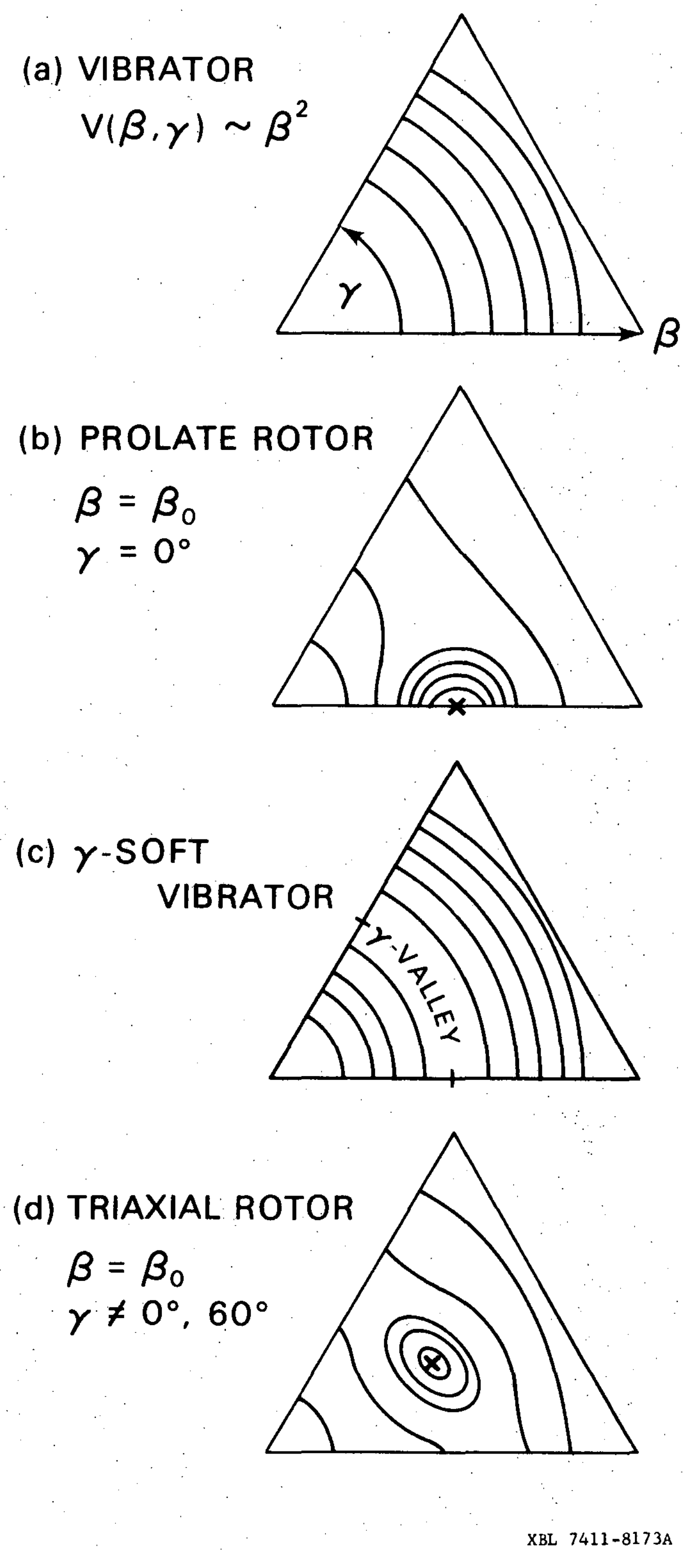
(a) VIBRATOR
$V(\beta,\gamma) \sim \beta^2$
γ
β
(b) PROLATE ROTOR
$\beta = \beta_0$
$\gamma = 0°$
(c) γ-SOFT
VIBRATOR
γ-VALLEY
(d) TRIAXIAL ROTOR
$\beta = \beta_0$
$\gamma \neq 0°, 60°$
XBL 7411-8173A

Fig. 10

TECHNICAL INFORMATION DIVISION
LAWRENCE BERKELEY LABORATORY
UNIVERSITY OF CALIFORNIA
BERKELEY, CALIFORNIA 94720